

Biomaterials Science

Accepted Manuscript

This article can be cited before page numbers have been issued, to do this please use: Y. Tsai, C. Chang and Y. Yeh, *Biomater. Sci.*, 2020, DOI: 10.1039/D0BM00632G.



This is an Accepted Manuscript, which has been through the Royal Society of Chemistry peer review process and has been accepted for publication.

Accepted Manuscripts are published online shortly after acceptance, before technical editing, formatting and proof reading. Using this free service, authors can make their results available to the community, in citable form, before we publish the edited article. We will replace this Accepted Manuscript with the edited and formatted Advance Article as soon as it is available.

You can find more information about Accepted Manuscripts in the [Information for Authors](#).

Please note that technical editing may introduce minor changes to the text and/or graphics, which may alter content. The journal's standard [Terms & Conditions](#) and the [Ethical guidelines](#) still apply. In no event shall the Royal Society of Chemistry be held responsible for any errors or omissions in this Accepted Manuscript or any consequences arising from the use of any information it contains.

Formation of highly elastomeric and property-tailorable poly(glycerol sebacate)-co-poly(ethylene glycol) hydrogels through thiol-norbornene photochemistry

Yu-Ting Tsai,^a Chun-Wei Chang^a and Yi-Cheun Yeh*^a

^a Institute of Polymer Science and Engineering, National Taiwan University, Taipei, Taiwan

E-mail: yicheun@ntu.edu.tw

Abstract

Poly(glycerol sebacate) (PGS) is a synthetic biorubber that presents good biocompatibility, excellent elasticity and desirable mechanical properties for biomedical applications; however, the inherent hydrophobicity and traditional thermal curing of PGS restrict its fabrication of hydrogels for advanced bioapplications. Here, we designed a new class of hydrophilic PGS-based copolymer that allows hydrogel formation through thiol-norbornene chemistry. Poly(glycerol sebacate)-co-polyethylene glycol (PGS-co-PEG) macromers were synthesized through a stepwise polycondensation reaction, and then the norbornene functional groups were introduced to PGS-co-PEG structure to form norbornene-functionalized PGS-co-PEG (Nor_PGS-co-PEG). Nor_PGS-co-PEG macromers can be crosslinked using dithiols to prepare hydrogels in the presence of light and photoinitiator. The mechanical, swelling and degradation properties of Nor_PGS-co-PEG hydrogels can be controlled by altering the crosslinker amount. In particular, the elongation of Nor_PGS-co-PEG hydrogels can be modulated up to 950%. Nor_PGS-co-PEG can be processed using electrospinning and 3D printing techniques to generate microfibrinous scaffolds and printed structures, respectively. In addition, the cytocompatibility of Nor_PGS-co-PEG was also demonstrated using *in vitro* cellular viability studies. These results indicate that Nor_PGS-co-PEG is a promising biomaterial with definable properties for scaffold manufacturing, presenting a great potential for biomedical applications.

Keywords: hydrogel, elastomer, biodegradable, photocrosslinking, thiol-norbornene chemistry

Introduction

Hydrogels are crosslinked polymer networks that can absorb large amounts of water or biological fluids. Hydrogels present biocompatibility, biodegradability and good mechanical tunability for various biological applications, such as drug delivery, biosensors and tissue implants.¹⁻⁶ In particular, hydrogels are promising materials for scaffold construction in tissue engineering, such as bone⁷, skin⁸ and cardiovascular^{9,10} regeneration. A variety of hydrophilic polymers, including synthetic polymers (e.g., polyethylene glycol¹¹) and natural polymers (e.g., alginate¹², hyaluronic acid³ and chitosan¹³) have been used as construct materials for hydrogels. To mimic the deformability of the extracellular matrix in many tissues, elastic hydrogels are highly desired in tissue engineering applications.

Poly(glycerol-sebacate) (PGS) is a biorubber that can be synthesized through the condensation reaction of glycerol and sebacic acid.¹⁴ PGS is a biocompatible materials with excellent elasticity, desirable mechanical properties and tunable biodegradability^{15,16}, making it a promising candidate in vascular regeneration^{17,18}, nerve regeneration¹⁹ and myocardial tissue engineering²⁰⁻²². The properties of PGS can be modulated by controlling reactant amounts and curing conditions to obtain a wide range of mechanical properties and degradation rates for different applications.¹⁴ However, the inherent hydrophobicity of PGS limits their expanding applications in biology, such as 3D encapsulation of cells.

To increase the hydrophilicity of PGS, citric acid has been incorporated within PGS backbone, where the existence of hydroxyl groups and ester bonds enhances the water uptake ability of poly(sebacate-glycerol-citrate) (PGSC).²³ In particular, the molecular weight and mechanical properties of the PGSC elastomers can be altered by varying the thermal curing time. Designing a polyether-polyester copolymer is another promising approach to improve the hydrophilicity of polyesters.²⁴ Polyethylene glycol (PEG) segment was incorporated within PGS backbone to obtain hydrophilic PGS-*co*-PEG copolymers.^{25,26} Thermal curing process can be applied to further crosslink PGS-*co*-PEG network, where FTIR spectra showed the decrease in the peak area of carboxyl and

hydroxyl group at 1350 and 1100 (and at 3400) cm^{-1} respectively and increase in ester group at 1150 cm^{-1} after the thermal crosslinking.²⁵ Nevertheless, these methods still require harsh curing conditions (i.e. high temperature and high vacuum environments) to obtain hydrophilic PGS copolymers for the preparation of hydrogels.

Several studies have demonstrated that PGS-*co*-PEG modified with different functional groups can be crosslinked to produce hydrogels under ambient conditions. For example, benzaldehyde-functionalized PGS-*co*-PEG has been synthesized, where 4-formylbenzoic acid (FA) was graft onto the polymer chain to form PEGS-FA. By blending the quaternized chitosan-g-polyaniline (QCSP) with PEGS-FA, an injectable, antibacterial, electroactive and anti-oxidant hydrogel has been developed for wound dressing.²⁷ Tyramine (TA) modified PGS-*co*-PEG can be crosslinked in the presence of horseradish peroxidase (HRP) and H_2O_2 , showing an enzyme-catalyzed *in situ* crosslinkable and injectable hydrogel.²⁸ Recently, a urethane-based PGS-*co*-PEG (PEGS-U) bioelastomer has been developed,²⁹ and its hydrophilicity and mechanical property are highly controllable with the synergistic effect of PEG and hexamethylene diisocyanate (HDI) content. PEGS-U was used to prepare polymer films, scaffolds and tubes for tissue engineering *via* solvent-free method. In addition, PEGS-U was applied as biocompatible materials to encapsulate and release proteins under mild crosslinking process. Methacrylated PGS-*co*-PEG has been developed to allow the use of ultraviolet (UV) light to crosslink the polymers, where the mechanical properties and biodegradation rate can be fine-tuned at varying the degree of methacrylation.³⁰

Here, we aim to introduce a photocurable group (i.e. norbornene) to PGS-*co*-PEG structure, allowing the formation of a new class of photocurable and elastomeric hydrogels through the photoinitiated thiol-norbornene reaction. Thiol-norbornene photochemistry have been applied in the formation of different classes of hydrogels based on their source, including hyaluronic acid³¹, gelatin³², alginate³³ and polyethylene glycol³⁴. Thiol-norbornene photochemistry is a step-growth reaction that generates uniform and controllable networks than the networks formed through chain-

growth polymerization.³⁴ Compared to free-radical polymerization of chain-growth reaction that can be inhibited by oxygen and results in an accumulation of reactive oxygen species (ROS), thiol-norbornene reaction is a free-radical step-growth polymerization that can consume ROS.³⁵ As excessive ROS disrupts the cellular homeostasis balance in biological system, thiol-norbornene reaction is a highly cytocompatible chemistry for biomaterial design.³⁶⁻³⁸ Furthermore, thiol-norbornene reactions perform a rapid gelation with lower concentration of photoinitiator and lower dosage of UV light compared to other crosslinkable mechanism.³⁹⁻⁴¹ Particularly, thiol-norbornene reaction is relatively not sensitive to oxygen inhibition, allowing the process of photocrosslinking under ambient conditions.⁴²

In this work, reactive norbornene groups were introduced to PGS-*co*-PEG structure to obtain norbornene-functionalized PGS-*co*-PEG (Nor_PGS-*co*-PEG). Nor_PGS-*co*-PEG macromers were crosslinked using 2,2'-(ethylenedioxy)diethanethiol through thiol-norbornene photochemistry to prepare hydrogels. The mechanical properties, swelling and degradation behaviors of Nor_PGS-*co*-PEG hydrogels can be simply tailored by changing the crosslinker amount, showing a much easier and straightforward strategy to fine-tune the properties of PGS-*co*-PEG hydrogels. Compared to the reported PGS-*co*-PEG system, which is a time-consuming process to change the properties of hydrogels by synthesizing several batches of PGS-*co*-PEG with different modification percentage of functional groups,³⁰ our strategy of using the crosslinker amount allows the use of the same batch of functionalized PGS-*co*-PEG to perform a range of properties. In addition, the elongation of Nor_PGS-*co*-PEG hydrogels can be adjusted up to 950%, which was greater than the current PGS-*co*-PEG hydrogels (~ 400%)^{25, 29} as well as our previous work of Nor-PGS (~ 250%)⁴⁰. Thus, Nor_PGS-*co*-PEG is a promising biomaterial to prepare highly stretchable hydrogels^{43, 44} for biomedical applications, such as wound dressing^{45, 46}, artificial tendons⁴⁷ and wearable sensors^{43, 48}. Given the PGS-*co*-PEG scaffolds have not been reported using biofabrication techniques, we demonstrated the processing ability of Nor_PGS-*co*-PEG using electrospinning and 3D printing to fabricate

microfibrinous scaffolds and 3D printed structures, respectively. Furthermore, *in vitro* cellular studies showed Nor_PGS-*co*-PEG hydrogels possessed good cytocompatibility. Particularly, Nor_PGS-*co*-PEG hydrogels provided a 3D environment for cell encapsulation, which was not able to be done in hydrophobic PGS systems,¹⁴ including our previous work of Nor-PGS.⁴⁰ Also, compared to Nor-PGS system, PEG segments provide the tunable hydration property of Nor_PGS-*co*-PEG to further determine the degradation rate of hydrogels. In addition, the ability of controllable biodegradation makes Nor_PGS-*co*-PEG hydrogels more attractive than PEG hydrogels for cell encapsulation applications. Taken together, these studies demonstrated that Nor_PGS-*co*-PEG is a promising photocurable and elastomeric biomaterials for biomedical applications.

Materials and methods

Materials

Polyethylene glycol (1000 g/mol) and glycerol (99+% pure) were purchased from Alfa Aesar. Sebacic acid (99% pure), 2,2'-(ethylenedioxy) diethanethiol (EDT, 95%) and 2-hydroxy-4'-(2-hydroxyethoxy)-2-methylpropiophenone (I2959, 98%) were supplied from Sigma-Aldrich. 1-Ethyl-3-(3-dimethylaminopropyl)carbodiimide hydrochloride (EDC·HCl, 99%) and 4-dimethylaminopyridine (DMAP, 99%) were purchased from Fluorochem. Dichloromethane (DCM) was purchased from Duksan and dried before use. For cell culture, dulbecco's modified eagle medium (DMEM, 4.5 g/L glucose), fetal bovine serum (FBS) and alamarBlue[®] assay were purchased from ThermoFisher, USA. Penicillin/streptomycin and 4-(2-hydroxyethyl)-1-piperazineethanesulfonic acid (HEPES) were supplied from Gibco, USA.

Synthesis and characterization of PGS-*co*-PEG and Nor_PGS-*co*-PEG

Poly(ethylene glycol)-*co*-poly(glycerol sebacate) (PGS-*co*-PEG), a multi-block copolymer, was synthesized by a modified procedure from the reported two-step condensation polymerization.¹⁴ The first step was the polycondensation reaction of polyethylene glycol (PEG) and sebacic acid (SAA). PEG (30 g, 0.03 mol) and SAA (8.09 g, 0.04 mol) were evenly mixed in a round-bottom flask at 130

°C under nitrogen flow for 2 h, and then a vacuum of 100 mTorr was applied for 24 h. In the second step of the polymerization, a given amount of glycerol (0.92 g, 0.01 mol) was added into the flask under the flow of nitrogen at 130 °C. The equivalents of dicarboxy acid is equal to the total equivalents of diol from PEG and glycerol, whereas molar ratio of PEG/glycerol was fixed to 75/25 to develop PGS-*co*-75PEG macromers. After the mixture was thoroughly mixed, the reaction was further carried out under vacuum for another 48 h. PGS-*co*-PEG pre-polymer was dissolved in DI water, dialyzed against DI water (Cellu-Sep T1 dialysis membrane, MWCO 3500 Da, MFPI, USA) for 3 days, and then lyophilized.

Norbornene-modified PGS-*co*-PEG was synthesized in the following steps: 5-norbornene-2-carboxylic acid (Nor-COOH) (0.15 g, 1.05 mmol) was dissolved in dry DCM (20 ml), and 4-dimethylaminopyridine (DMAP) (0.13 g, 1.05 mmol), PGS-*co*-PEG macromers (2 g) and EDC·HCl (1.00 g, 5.25 mmol) were further added into the flask. The mixture was stirred at 37 °C under nitrogen condition for 72 h. After the reaction, DCM was removed and the products were dissolved in DI water and dialyzed for 3 days before lyophilization.

Gel permeation chromatography (GPC), nuclear magnetic resonance (NMR) spectroscopy and Fourier-transform infrared (FTIR) spectroscopy were used to characterize polymers. The molecular weight of polymers was measured using GPC. (ESI, Fig. S1) Polymers were dissolved in tetrahydrofuran (THF) at a concentration of 5 mg/mL. GPC was performed using Enshine SUPER CO-150, where a set of two polystyrene gel columns (Styragel HR 2 and Styragel HR 4) was used for separation, and polystyrene standards were used for calibration. ¹H NMR (400 MHz) spectra of polymers were obtained using Bruker AVIII HD 400 NMR, with deuterium oxide (D₂O) as the solvent and chemical shifts (δ) were referenced to δ 4.8 ppm. PEG content in PGS-*co*-PEG structure was calculated by following the reported method using NMR spectra.^{25, 49} Signals at 6.26-5.88 ppm contributed from the vinyl protons (–CH=CH–) of norbornene groups were used for the calculation of the modification percentage of norbornene in PGS-*co*-PEG structure. FTIR spectra of polymers

were obtained with Alpha Bruker spectrometer in the range of 650-4000 cm^{-1} over 8 scans.

Rheological measurement

Nor_PGS-co-PEG macromers (30 wt%) were mixed with EDT (norbornene/thiol= 1) and I2959 (0.05 wt%) in PBS for hydrogel formation. Dynamic oscillatory time sweeps were performed using a stress-controlled rheometer (Discovery HR-2 model, TA Instruments, USA) with an UV light guide accessory (SmartSwap™, TA Instruments) connected to an UV light source (Omicure S1500, EXFO, USA). Nor_PGS-co-PEG was crosslinked under the exposure of UV light (365 nm, 10 mW/cm^2). Storage (G') and loss (G'') moduli with time were monitored under 0.5% strain and 1 Hz, using a cone and plate geometry (59 min 42 s (0.995°) cone angle, 20 mm diameter, 250 μm gap) at room temperature.

Preparation of Nor_PGS-co-PEG hydrogels

Nor_PGS-co-PEG macromers was dissolved in phosphate buffered saline (PBS, pH 7.4) in the presence of EDT as a crosslinker and I2959 (0.05 wt%) as a photoinitiator. The mixture was crosslinked to form a hydrogel under UV light (365 nm, 10 mW/cm^2 , 3 min).

Swelling of Nor_PGS-co-PEG hydrogels

Nor_PGS-co-PEG hydrogels were lyophilized and weighed (w_1). The freeze-dried hydrogels were placed in PBS at 37 °C with 100 r.p.m. shaking speed on a digital rotator for 9 h until the water equilibrium was reached. Gently wiped the excess PBS on hydrogel surface and immediately weighed to get the wet weight (w_2) of hydrogel. The equilibrium swelling ratio and equilibrium water uptake of hydrogels were calculated using the following equations:

$$\text{Equilibrium swelling ratio} = w_2/w_1$$

$$\text{Equilibrium water content (\%)} = (w_2-w_1)/w_2 \times 100\%$$

Degradation of Nor_PGS-co-PEG

Freeze-dried Nor_PGS-co-PEG hydrogels with known weight (w_0) were soaked in NaOH (0.01 N) or PBS (pH 7.4) solutions at 37 °C with 100 r.p.m. shaking speed on a digital rotator to monitor the

degradation of Nor_PGS-*co*-PEG hydrogels. The samples were taken out at each scheduled time point, and then rinsed with DI water before lyophilization. The weight (w_d) of hydrogels was measured, and the percentage of mass remaining was calculated by $w_d/w_0 \times 100\%$.

Compression and tensile testing of Nor_PGS-*co*-PEG

Mechanical properties of Nor_PGS-*co*-PEG hydrogels were evaluated by compression and tensile testing using the instrument of Materials Testing System (MTS) installed with 250 N load cell. The compression properties were measured at the crosshead speed of 10 mm/min and the tensile testing were at 30 mm/min. For compression test, hydrogels were cast into 5 mm diameter cylinders; for tensile testing, hydrogels were cast into dog-bone shaped samples using polydimethylsiloxane (PDMS) molds (1.3 mm thick, 5.0 mm width at center). Force-displacement curves obtained from the machine were converted to stress-strain curves. Young's modulus was calculated from the linear stress-strain region by fitting a straight line between 15% and 30% strain, while the tensile modulus was measured by determining the slope between 40% and 60% strain.

Fabrication of Nor_PGS-*co*-PEG scaffolds using electrospinning and 3D printing

Nor_PGS-*co*-PEG (30 wt%), EDT (thiol/norbornene = 1), I2959 (0.05 wt%) and polyethylene oxide (PEO, $M_w = 900$ kDa, 3.5 wt%) were mixed in ethanol (90%) for electrospinning. The materials were electrospun at 0.4 kV/cm and 0.42 mL/h flow rate with 21 gauge needle, and then collected on a foil covered plate. Collected fibrous matrix was irradiated under UV light (365 nm, 10 mW/cm²) for 10 min. Fibers were imaged using scanning electron microscopy (SEM, Hitachi TM-3000 system).

Nor_PGS-*co*-PEG macromers (30 wt%), EDT (thiol/norbornene = 1) and I2959 (0.05 wt%) were mixed in PBS (pH 7.4) for printing. An extrusion-based 3D printer (Tissue Scribe 3D bioprinter, 3D Cultures company, USA) was used in the printing of Nor_PGS-*co*-PEG. The materials were loaded into a syringe with affixed blunt tip 25 G needles that were 13 mm long. Syringes were loaded onto the 3D printer and the printing was performed with continuous UV irradiation (365 nm, 10 mW/cm²) of the print area during printing.

Cellular studies

Mouse embryo fibroblasts (MEF) were harvested from C57BL/6N mice embryo and then immortalized after 15 passages. MEFs were incubated at 37 °C under 5% CO₂ with humidified atmosphere in DMEM containing 10% FBS, 1% penicillin/streptomycin, and 1% HEPES. Cells were subcultured twice weekly. For 2D cell culture, MEFs were seeded on a photocrosslinked hydrogel surface (2×10^6 cells/mL); for 3D cell culture, MEFs were encapsulated within hydrogel (2×10^6 cells/mL) and mould into syringe with 50 μ L volumes before UV irradiation (365 nm, 10 mW/cm², 3 min). Hydrogels were incubated in DMEM supplemented with 10% fetal bovine serum (FBS), 1% penicillin/streptomycin and 1% HEPES.

Live/Dead staining and cell metabolism assay were performed to evaluate the cell viability of MEFs. For Live/Dead staining, MEFs were characterized through fluorescent staining of live cells as green (2 μ M calcein-Am, Invitrogen) and dead cells in red (4 μ M ethidium homodimer-1, Invitrogen). Cell-encapsulated hydrogels were incubated at 37 °C under 5% CO₂, rinsed with PBS, and then observed using Leica SP5 confocal microscopy at day 1. Images were analyzed with Image J (NIH). Metabolic activity of MEFs was measured using alamarBlue[®] assay followed the manufacturer instructions, where the samples were incubated in alamarBlue solutions (10% in serum-contained media) for 4 h. Quantification at each time point was performed on a microplate reader (Multi-Detection Microplate Reader, BioTek Synergy HT) at an excitation of 530 nm and emission of 590 nm, and the values were normalized to readings at day 1 (D1) for each sample.

Statistical analysis

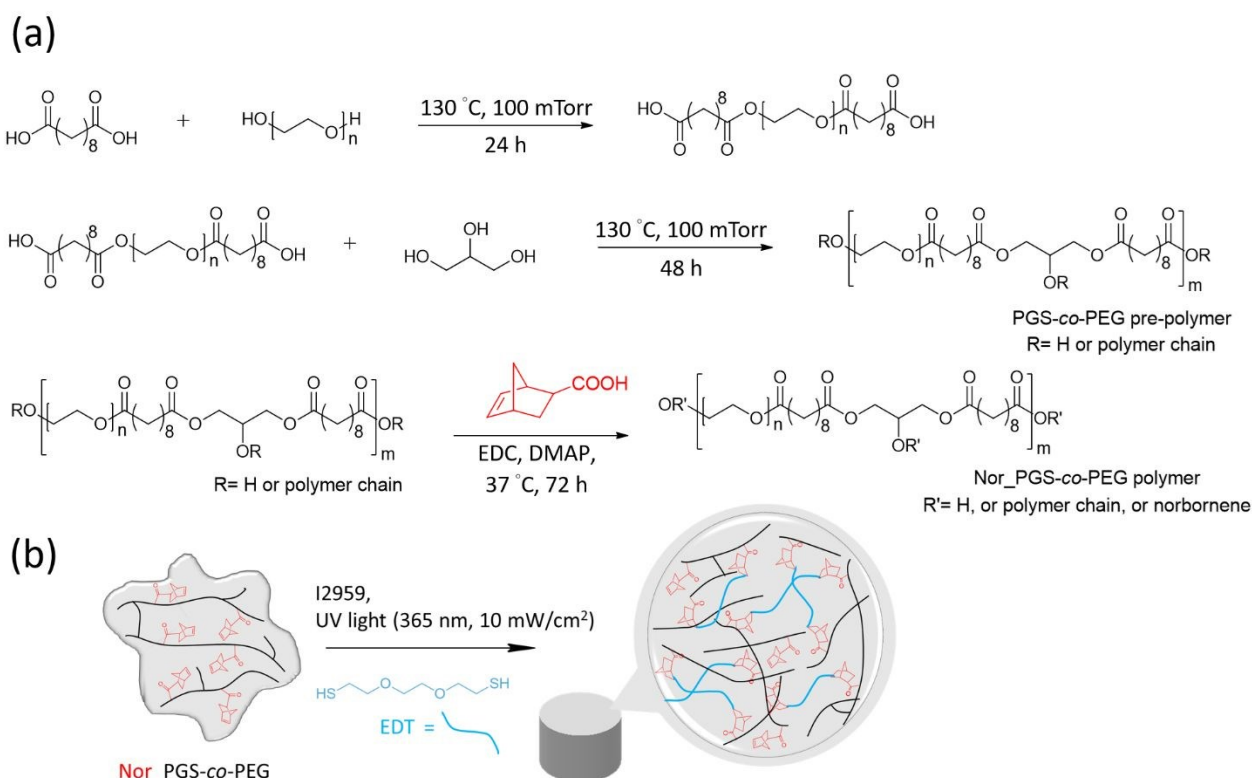
All experiments were performed with three replicates. Error bars were reported in figures as the standard deviation (s.d.) unless otherwise noted. The t-test analysis was used to determine statistical significance of differences in the data analysis. Significance was set at $p < 0.05$ with *, ** or *** indicating $p < 0.05$, 0.01 or 0.001, respectively.

Results and discussion

Design and characterization of Nor_PGS-*co*-PEG

PGS-*co*-PEG has been reported as an elastic, biocompatible and biodegradable copolymer for biomedical applications. However, the thermal curing process of PGS-*co*-PEG required harsh conditions to obtain the crosslinked polymer. Functionalization of PGS-*co*-PEG is a promising strategy to control the properties of PGS-*co*-PEG as well as process PGS-*co*-PEG into complex structures.²⁷⁻³⁰ Here, we introduce a new functional group (i.e. norbornene) to PGS-*co*-PEG structure to allow the formation of PGS-*co*-PEG hydrogels *via* thiol-norbornene crosslinking, providing a simple approach to fine-tune the properties of PGS-*co*-PEG as well as fabricate 3D scaffolds of PGS-*co*-PEG.

In this study, PGS-*co*-PEG was synthesized *via* a stepwise polycondensation reaction. Sebacic acid and polyethylene glycol were reacted at 130 °C and 100 mTorr for 24 h to synthesize poly(ethylene glycol)-sebacic acid polyester, and then glycerol was added to the mixture to form PGS-*co*-PEG macromers after a reaction of 48 h. (**Scheme 1a, top**) Hydroxyl groups of PGS-*co*-PEG were then reacted with 5-norbornene-2-carboxylic acid to obtain norbornene-functionalized PGS-*co*-PEG (Nor_PGS-*co*-PEG). (**Scheme 1a, bottom**) Nor_PGS-*co*-PEG macromers (M_w= 9.6 kDa, PDI= 2.71) can be crosslinked using 2,2'-(ethylenedioxy) diethanethiol (EDT) as the crosslinkers in the presence of photoinitiator (I2959, 0.05 wt%) under UV light (365 nm, 10 mW/cm²). (**Scheme 1b**)



Scheme 1 (a) Synthetic process of PGS-co-PEG and Nor_PGS-co-PEG. (b) Schematic illustration of the crosslinking of Nor_PGS-co-PEG macromers using EDT as crosslinkers in the presence of I2959 and UV light.

PGS-co-PEG and Nor_PGS-co-PEG were characterized using NMR and FTIR spectroscopies. In the ^1H NMR spectra of PGS-co-PEG macromers (**Fig.1a, top**), signals at 1.30 ppm (peak 5), 1.52 ppm (peak 4) and 2.35 ppm (peak 3) were recognized as the methylene protons ($-\text{COCH}_2\text{CH}_2\text{CH}_2-$) of sebacic acid, and signal at 3.62 ppm (peak 6) corresponded to the methylene protons ($-\text{COCH}_2\text{CH}_2\text{O}-$) of PEG segments. Peaks between 3.5-5.2 ppm (peak 1, 2) attributed to the methylene protons ($-\text{CH}_2\text{CH}-$) of glycerol. In the ^1H NMR spectra of Nor_PGS-co-PEG (**Fig.1a, bottom**), signals at 6.26-5.88 ppm (peak a, b) assigned to the vinyl protons ($-\text{CH}=\text{CH}-$) of norbornene groups, indicating norbornene groups were grafted onto the PGS-co-PEG structure. The PEG content and the modification percentage of norbornene groups in PGS-co-PEG structure were calculated using ^1H NMR spectra, showing ~75% of PEG content and ~80% of norbornene modification in the structure.

In the FTIR spectra, the peaks at 1730 cm^{-1} and 1150 cm^{-1} corresponded to the C=O stretch and C-O-C stretch of the ester groups in the PGS-*co*-PEG structure. **(Fig.1b)** The strong and broad band covering a wide range between 3300 and 3700 cm^{-1} corresponded to the O-H stretch, which was majorly contributed from the water within PEG segment in the PGS-*co*-PEG structure. Therefore, the O-H band did not disappear after modification with norbornene as it still presented in the FTIR spectra of Nor_PGS-*co*-PEG. Additionally, comparing the FTIR spectra between PGS-*co*-PEG and Nor_PGS-*co*-PEG, the appearance of a new peak at 3020 cm^{-1} corresponded to the vinyl group from norbornene, indicating Nor_PGS-*co*-PEG has been successfully synthesized.

Photocrosslinking of Nor_PGS-*co*-PEG macromers was investigated using rheology, where the norbornenes on Nor_PGS-*co*-PEG macromers were crosslinked by EDT through thiol-norbornene reaction. Rheology showed a rapid crosslinking of Nor_PGS-*co*-PEG macromers in the presence of photoinitiator (I2959, 0.05 wt%) and UV light (365nm , 10 mW/cm^2), where the gel point can be observed within seconds and a plateau modulus was reached within ~ 3 min. **(Fig. 1c)**

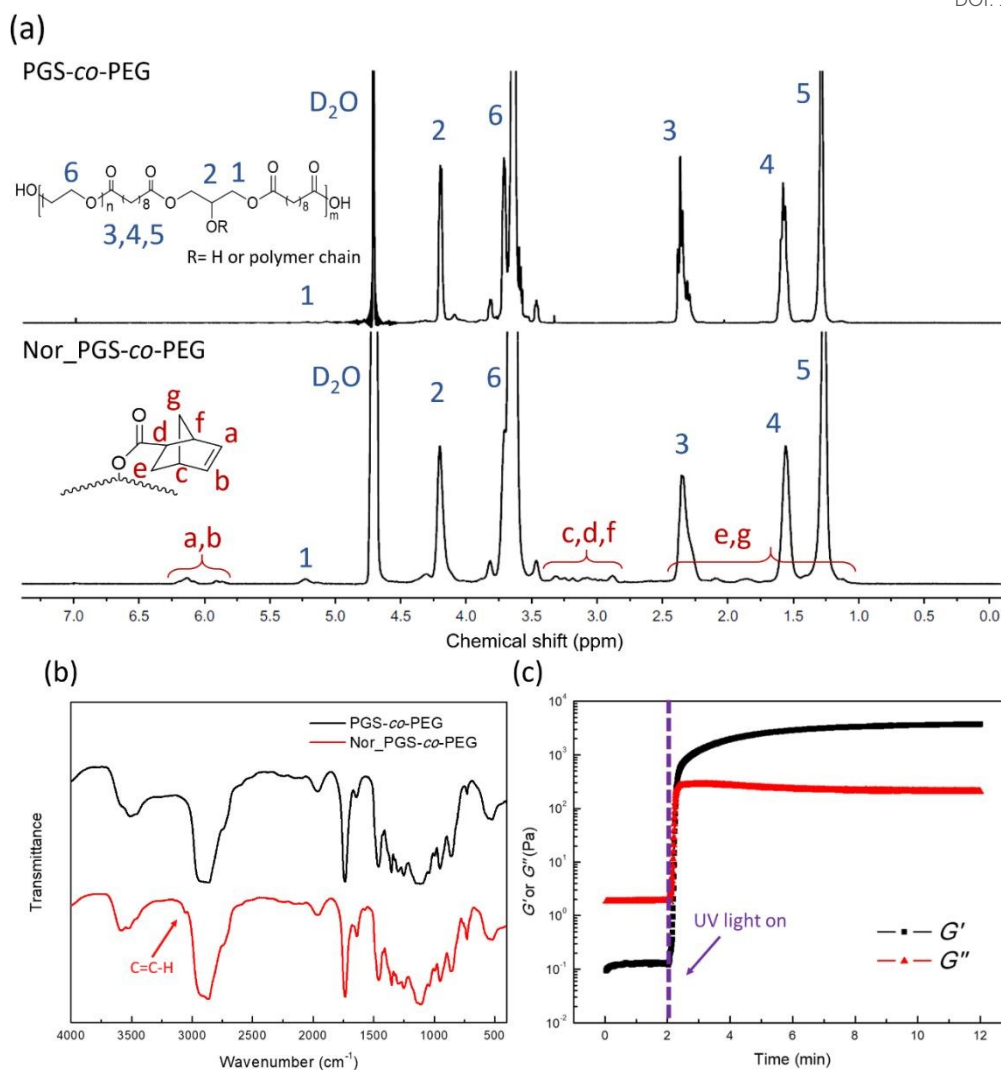


Fig. 1 (a) ¹H NMR spectra of PGS-co-PEG (top) and Nor_PGS-co-PEG (bottom). (b) FTIR spectra of PGS-co-PEG and Nor_PGS-co-PEG. (c) Rheology of the photocrosslinking of Nor_PGS-co-PEG hydrogels under UV irradiation.

Nor_PGS-co-PEG hydrogels exhibit tunable properties

Nor_PGS-co-PEG hydrogels presented Young's modulus of 5.30, 13.04 and 27.10 kPa for 20 wt%, 30 wt% and 40 wt% of materials, respectively. (**Fig. 2a**) In addition, Nor_PGS-co-PEG hydrogels (30 wt%) were prepared with several thiol/norbornene ratios ($N= 0.65, 0.85$ and 1), and the mechanical properties of Nor_PGS-co-PEG hydrogels were determined with compression and tensile testing. The Young's modulus of Nor_PGS-co-PEG hydrogels was adjusted by the EDT amount used for photocrosslinking, showing 6.9, 11.2 and 16.5 kPa for $N= 0.65, 0.85$ and 1, respectively. (**Fig. 2b**) These results showed the compression properties of Nor_PGS-co-PEG hydrogels can be easily fine-

tuned by adding different amount of crosslinker. On the other hand, Nor_PGS-*co*-PEG hydrogels of $N= 1.33$ showed a lower Young's modulus (5.9 kPa) compared to the $N= 1$ sample, indicating the excessive amount of thiolated crosslinker presented lower crosslinking density in hydrogels as some dithiols only reacted with one norbornene and few free thiols were remaining in the hydrogels.^{32, 50}

PGS-*co*-PEG have been demonstrated as an elastomeric block copolymer.²⁵ Here, Nor_PGS-*co*-PEG hydrogels also performed excellent elasticity. Repetitive compression loading of Nor_PGS-*co*-PEG hydrogels showed that the loading curves did not change in moduli between loading cycles.

(Fig. 2c)

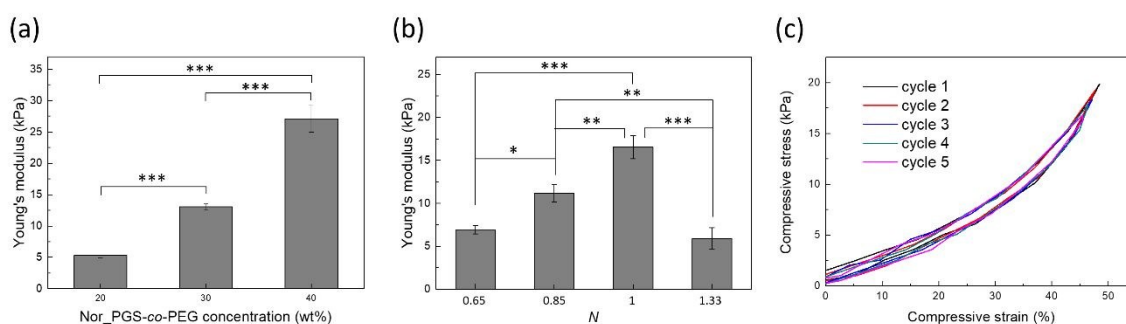


Fig. 2 Compressive properties of Nor_PGS-*co*-PEG hydrogels with (a) different weight percentages and (b) different amounts of crosslinker. (c) Nor_PGS-*co*-PEG hydrogels ($N= 1$) under repetitive compression loading to 50% strain (five cycles at a crosshead speed of 10 mm/min). Significance was set at $p < 0.05$ with *, ** or *** indicating $p < 0.05$, 0.01 or 0.001, respectively.

In tensile testing, Nor-PGS-*co*-PEG samples with varied thiol/norbornene ratios were also investigated. The % elongation of Nor-PGS-*co*-PEG hydrogels presented ~600%, ~800% and ~950% elongation for $N= 1$, 0.85 and 0.65, respectively. (Fig. 3a and 3b) Additionally, enhancement of Nor-PGS-*co*-PEG moduli with higher thiol/norbornene ratio resulted in greater failure stress and lower failure strain. (Fig. 3c-3e)

These compression and tensile results showed the mechanical properties of Nor_PGS-*co*-PEG hydrogels can be easily fine-tuned by adding different amount of crosslinker. Stronger mechanical properties of Nor_PGS-*co*-PEG network can be achieved by controlling the crosslinker amount to $N= 1$, while decreasing thiol/norbornene ratio resulted in a soft Nor_PGS-*co*-PEG network with high

elongation of over 900%. The elongation of Nor_PGS-*co*-PEG hydrogels was greater than the reported PGS-*co*-PEG hydrogels, which presented the elongation range lower than 400%.^{25, 29} Based on these mechanical results, Nor_PGS-*co*-PEG hydrogels possessed excellent elastic recovery and great ductility to be used as highly stretchable biomaterials for biomedical applications.

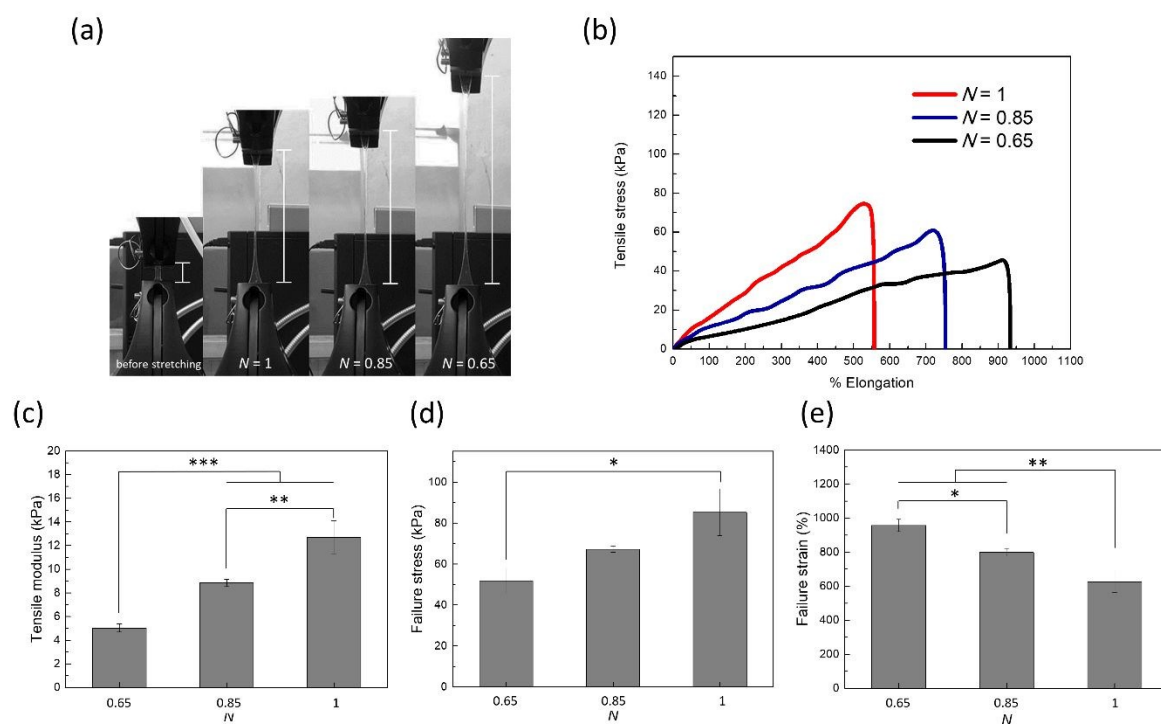


Fig. 3 Tensile properties of Nor_PGS-*co*-PEG hydrogels. (a) Representative images of samples before and after tensile loading, with images taken immediately before failure. (b) Representative tensile stress and elongation profiles of samples. (c) Tensile modulus, (d) failure stress and (e) failure strain of samples. N = thiol/norbornene ratio. Significance was set at $p < 0.05$ with *, ** or *** indicating $p < 0.05$, 0.01 or 0.001, respectively.

The crosslinked networks of hydrogels directly correlated with water uptake, where high water content of hydrogels can maintain the viability and function of the encapsulated cells.⁵¹ As-prepared Nor_PGS-*co*-PEG hydrogels with $N=0.65$, 0.85 and 1 yielded a swelling ratio of ~ 5.6 , ~ 4.4 and ~ 3.8 , respectively. (**Fig. 4a**) The trend of the swelling ratio was attributed to the crosslinking density of Nor_PGS-*co*-PEG hydrogels, where a higher thiol/norbornene ratio resulted in a higher crosslinking density.⁵² Furthermore, the equilibrium water content was above 70% for all hydrogels with different thiol/norbornene ratios. (**Fig. 4b**).

Previous studies have reported that the degradation of PGS-*co*-PEG was based on the hydrolysis of ester bond in their structures.^{14, 25} Here, degradability of Nor_PGS-*co*-PEG hydrogels was demonstrated in NaOH or PBS solutions. In NaOH solutions, Nor_PGS-*co*-PEG presented a fast degradation rate, where the mass loss of the $N=1$ sample was up to 45% and 70% after incubations for 1 h and 4 h, respectively. (**Fig. 4c**) In PBS solutions, Nor_PGS-*co*-PEG ($N=1$) was degraded by 17%, 25% and 30% after incubation in PBS solutions for 3, 5 and 7 days, respectively. (**Fig. 4d**) Obviously, the degradation of Nor_PGS-*co*-PEG hydrogels in PBS solutions was much slower than that in NaOH solutions. Most importantly, the degradation rate of Nor_PGS-*co*-PEG hydrogels in both conditions can be further controlled by changing the thiol/norbornene ratio, with the mass loss of the $N=0.65$ sample was the greatest among the $N=0.85$ and $N=1$ groups during the incubation time points. The fast degradation of the lower crosslinked Nor_PGS-*co*-PEG hydrogel was correlated with its higher water uptake behavior to accelerate the hydrolysis of the polymeric networks.²⁵ These results indicated that reducing the crosslinker amounts to decrease the crosslinking density in Nor_PGS-*co*-PEG networks presented a faster degradation, providing a varied lifetime of Nor- PGS-*co*-PEG hydrogels for different specific applications.

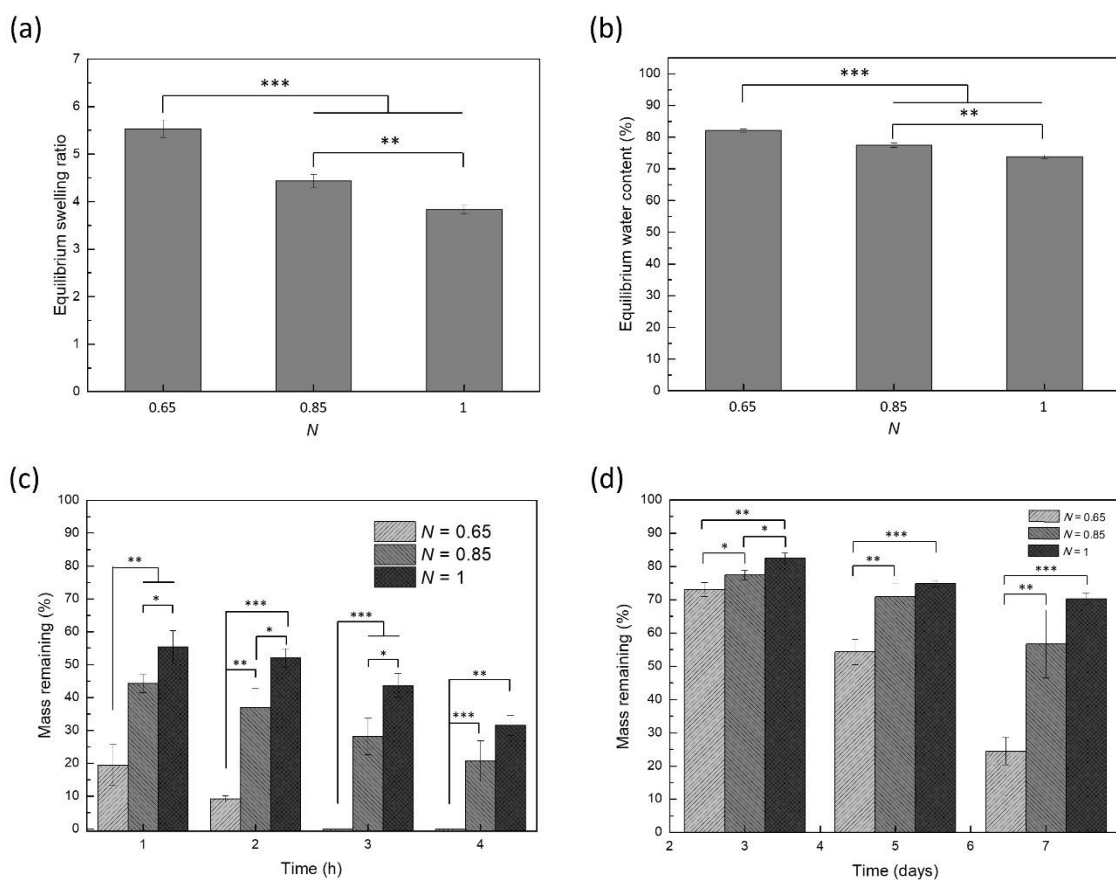


Fig. 4 Swelling and degradation properties of Nor_PGS-co-PEG. (a) Equilibrium swelling ratio and (b) equilibrium water content of Nor_PGS-co-PEG hydrogels with different thiol/norbornene ratios. Degradation of Nor_PGS-co-PEG hydrogels with different thiol/norbornene ratios in (c) NaOH (0.01 N) and (d) PBS (pH 7.4) solutions. Significance was set at ** or *** indicating $p < 0.01$ or 0.001 , respectively.

Nor_PGS-co-PEG for the fabrication of microfibrillar scaffolds and 3D printed structures

Processing Nor_PGS-co-PEG into scaffolds was demonstrated using electrospinning and 3D printing techniques. Nor_PGS-co-PEG (30 wt%), EDT (thiol/norbornene = 1), I2959 (0.05 wt%) and polyethylene oxide (PEO, 3.5 wt%) were mixed in ethanol (90%) for electrospinning, where PEO was used as a carrier polymer to adjust the viscosity as well as improve fiber formation. Furthermore, an additional electric field was set up around the collector of the electrospinning equipment, providing the ability to align fibers. Electrospun scaffolds were crosslinked using UV light (365 nm, 10 mW/cm²) to prevent dissolution in water. (ESI, Movie S1 and S2) SEM images of electrospun hybrid

Nor_PGS-*co*-PEG/PEO microfibrous scaffolds presented fiber diameters about $2.34 \pm 0.49 \mu\text{m}$. (**Fig. 5**) For 3D printing, Nor_PGS-*co*-PEG (30 wt%) along with EDT (thiol/norbornene= 1) and I2959 (0.05 wt%) was used as a photocurable ink for extrusion-based printing. The printing ability of Nor_PGS-*co*-PEG was demonstrated by printing a ring structure and a rectangular grid pattern in a layer-by-layer deposition process under continuous UV irradiation (365nm, 10mW/cm²). The ring structure was printed with 12 layers at a speed of 14 mm/s under room temperature, with a height of 2.4 mm, an outer diameter of 10.8 mm, and an inner diameter of 10 mm. (**Fig. 6a-6c**) The rectangular grid pattern was printed with 2 layers at a speed of 20 mm/s, showing the uniform filament width of 0.82 mm and spacing of 5 mm. (**Fig. 6d-6f**)

A number of studies have fabricated PGS scaffolds using electrospinning^{49, 53} and 3D printing^{40, 54}. However, to the best of our knowledge, PGS-*co*-PEG scaffolds have not been reported using biofabrication techniques. Here, we successfully demonstrated the processing ability of Nor_PGS-*co*-PEG using both electrospinning and 3D printing techniques. Introduction of norbornene groups to PGS-*co*-PEG structures allows the control of PGS-*co*-PEG crosslinking using thiol-norbornene photochemistry. Thus, Nor_PGS-*co*-PEG can be used as a photocurable material in the fabrication processes and applications. Compared to traditional thermal crosslinking of PGS-*co*-PEG that limits its processing in the fabrication of scaffolds, this post-synthesis photocrosslinking of Nor_PGS-*co*-PEG provides a promising approach to process PGS-*co*-PEG under ambient conditions, allowing a wide range of manufacturing techniques to be utilized in the future.

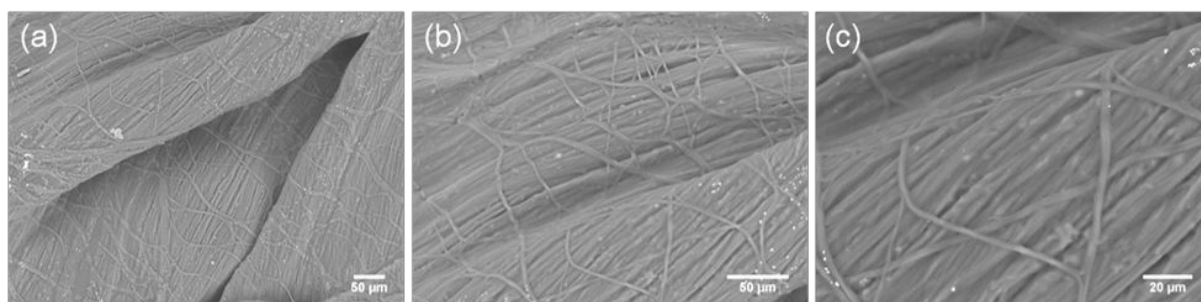


Fig. 5 SEM images of hybrid Nor_PGS-*co*-PEG/PEO microfibrous scaffolds in different magnifications of (a) 250x, (b) 500x and (c) 1000x.

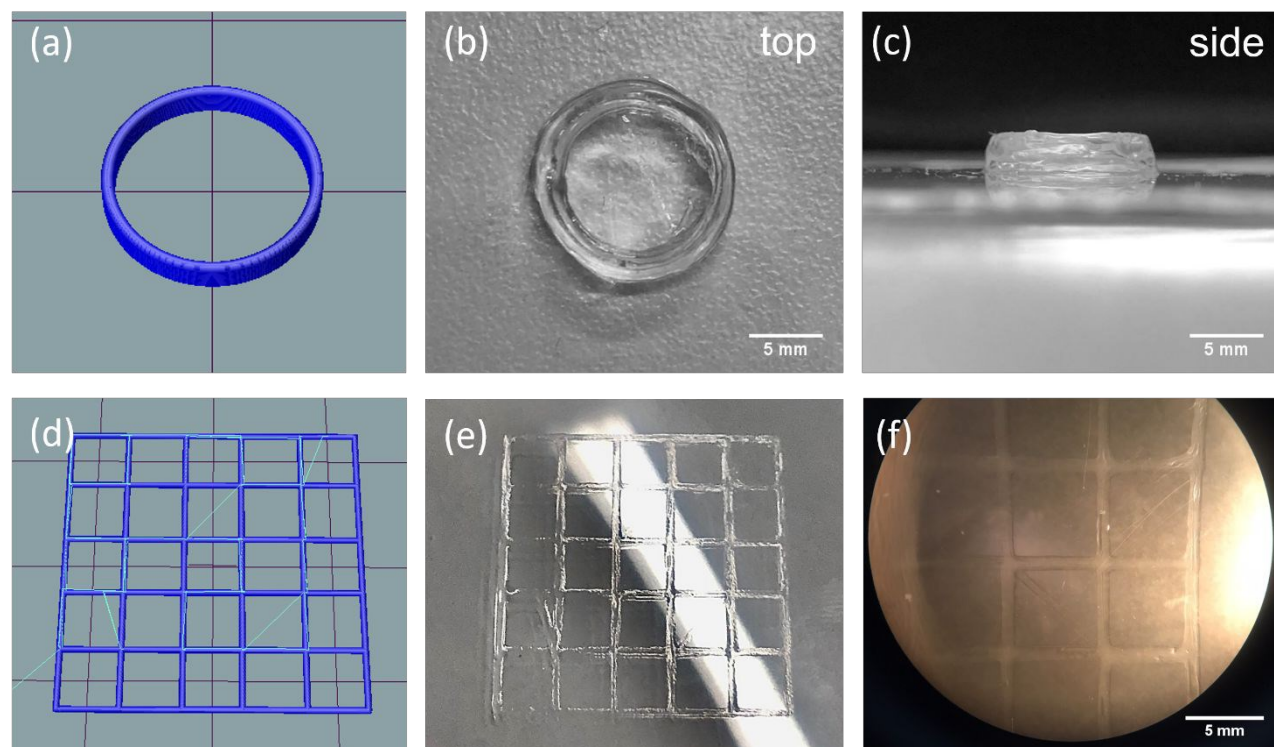


Fig. 6 Images of 3D printed scaffolds using Nor_PGS-*co*-PEG hydrogels. The 3D model of a ring structure (a), and the top view (b) and side view (c) of the printed structure. The 3D model of a rectangular grid pattern (d), and the top view (e, f) of the printed structure where (f) is the image taken with a microscope.

***In vitro* cytocompatibility study**

Cytocompatibility of Nor_PGS-*co*-PEG hydrogels was investigated using 2D and 3D cell cultures *in vitro*. Mouse embryonic fibroblasts (MEFs) were seeded on the surfaces of Nor_PGS-*co*-PEG hydrogels for 2D cell culture, while MEFs were encapsulated within hydrogels for 3D cell culture. Live/Dead staining was used to identify live and dead cells on both 2D and 3D culture conditions, where calcein-AM stained live cells green while ethidium homodimer-1 stained dead cells red. (**Fig. 7a** and **7b**) In addition, cellular metabolism was evaluated using an alamarBlue assay, showing the cellular metabolism of MEFs increased over time. (**Fig. 7c** and **7d**) The proliferation of cells in the PGS-*co*-PEG hydrogels has been shown in previous reports.^{25, 29, 30} Here, these results also

demonstrated that Nor_PGS-*co*-PEG hydrogels supported cell proliferation, and the thiol-norbornene reaction within the hydrogels was cytocompatible.

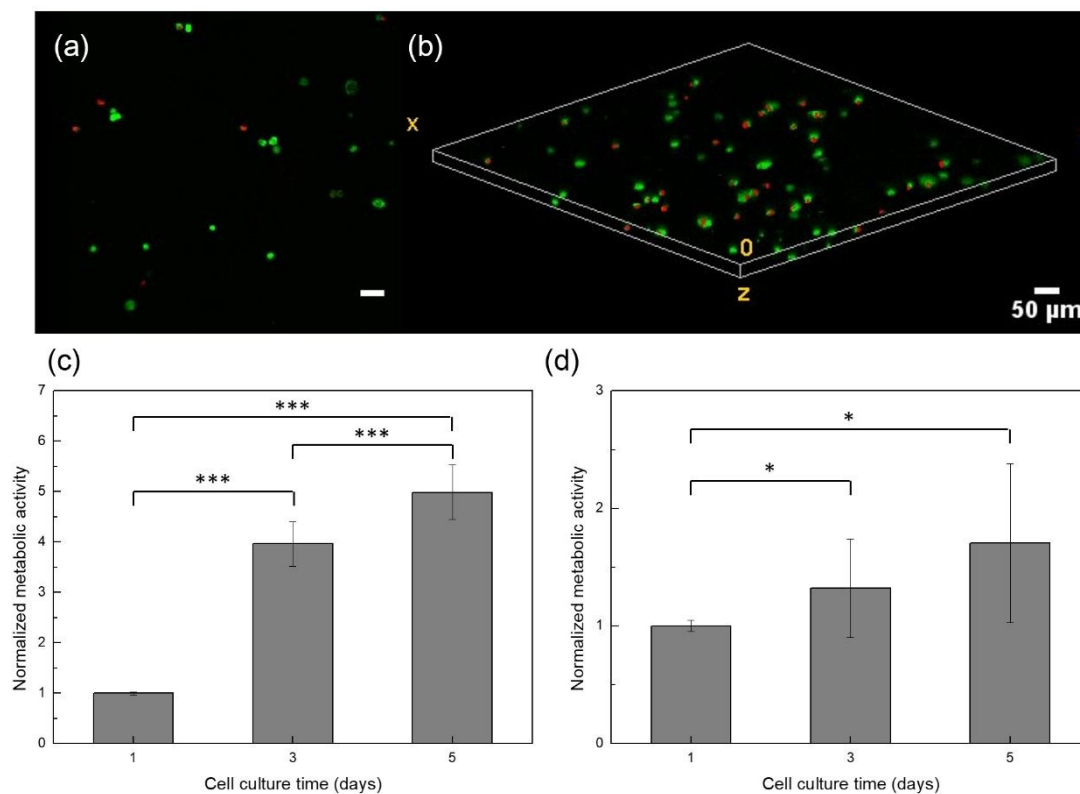


Fig. 7 Live/Dead staining and normalized metabolic activity of MEFs (a, c) on the surfaces of Nor_PGS-*co*-PEG hydrogels and (b, d) within the Nor_PGS-*co*-PEG hydrogels. There were six gels investigated in the metabolic activity experiments, and the values at day 3 and day 5 were normalized to the value at day 1. Significance was set at $p < 0.05$ with *, ** or *** indicating $p < 0.05$, 0.01 or 0.001, respectively.

Conclusions

Here we synthesized a new type of photocurable and elastomeric hydrogels using Nor_PGS-*co*-PEG. The norbornene functional groups on PGS-*co*-PEG allow the crosslinking of hydrogels *via* thiol-norbornene photochemistry. Several properties (i.e. mechanical property, swelling ratio and degradation rate) of Nor_PGS-*co*-PEG hydrogels can be simply modulated using different amounts of dithiols. The excellent elongation property (~950%) of Nor_PGS-*co*-PEG makes it as a promising stretchable biomaterial for applications in artificial organs, wound dressing and wearable

sensors. Also, Nor_PGS-co-PEG hydrogels have been successfully demonstrated in the fabrication of microfibrinous scaffolds and 3D printed structures, expanding the utility of PGS-co-PEG materials in biomedical field using biofabrication techniques. In addition, *in vitro* cellular studies showed that Nor_PGS-co-PEG hydrogels were cytocompatible. Taken together, Nor_PGS-co-PEG is an elastomeric biomaterial that presents unique and highly tailorable properties as well as performs 3D cell encapsulation, providing an ideal model to investigate the interaction mechanisms between the extracellular matrix and cells in biomedical applications.

Conflicts of interest

There are no conflicts to declare.

Acknowledgements

The authors would like to thank Prof. Wen-Chang Chen (Department of Chemical Engineering, National Taiwan University) for the help of GPC characterization, as well as Prof. Pen-hsiu Grace Chao (Department of Biomedical Engineering, National Taiwan University) for the assistance with electrospinning experiment and cellular studies. We thank Ms. S.-L. Huang (Ministry of Science and Technology, National Taiwan University) for the assistance in NMR experiments. This work was supported by the Ministry of Science and Technology, Taiwan (MOST-107-2113-M-022-025-MY4) and National Taiwan University (108PNTUS02 and 109PNTUS07).

ReferencesUncategorized References

1. M. W. Tibbitt and K. S. Anseth, *Biotechnol. Bioeng.*, 2009, **103**, 655-663.
2. N. Annabi, A. Tamayol, J. A. Uquillas, M. Akbari, L. E. Bertassoni, C. Cha, G. Camci-Unal, M. R. Dokmeci, N. A. Peppas and A. Khademhosseini, *Adv. Mater.*, 2014, **26**, 85-124.
3. J. A. Burdick and G. D. Prestwich, *Adv. Mater.*, 2011, **23**, H41-H56.
4. P. M. Kharkar, K. L. Kiick and A. M. Kloxin, *Chem. Soc. Rev.*, 2013, **42**, 7335-7372.
5. N. Oliva, J. Conde, K. Wang and N. Artzi, *Acc. Chem. Res.*, 2017, **50**, 669-679.
6. R. Rai, M. Tallawi, A. Grigore and A. R. Boccaccini, *Prog. Polym. Sci.*, 2012, **37**, 1051-1078.
7. Y. Zhao, Z. Cui, B. Liu, J. Xiang, D. Qiu, Y. Tian, X. Qu and Z. Yang, *Adv. Healthc.*

- Mater.*, 2019, **8**, 1900709.
8. S. P. Miguel, M. P. Ribeiro, H. Brancal, P. Coutinho and I. J. Correia, *Carbohydr. Polym.*, 2014, **111**, 366-373.
 9. A. J. Rufaihah and D. Seliktar, *Adv. Drug Deliv. Rev.*, 2016, **96**, 31-39.
 10. L. Millon, H. Mohammadi and W. Wan, *J. Biomed. Mater. Res. Part B Appl. Biomater.*, 2006, **79**, 305-311.
 11. S. J. Bryant and K. S. Anseth, *J. Biomed. Mater. Res. A*, 2003, **64**, 70-79.
 12. J. A. Rowley, G. Madlambayan and D. J. Mooney, *Biomaterials*, 1999, **20**, 45-53.
 13. J. Berger, M. Reist, J. M. Mayer, O. Felt, N. Peppas and R. Gurny, *Eur. J. Pharm. Biopharm*, 2004, **57**, 19-34.
 14. Y. Wang, G. A. Ameer, B. J. Sheppard and R. Langer, *Nat. Biotechnol.*, 2002, **20**, 602.
 15. X. J. Loh, A. A. Karim and C. Owh, *J. Mater. Chem. B*, 2015, **3**, 7641-7652.
 16. O. Valerio, M. Misra and A. K. Mohanty, *ACS Sustain. Chem. Eng.*, 2018, **6**, 5681-5693.
 17. J. Gao, P. M. Crapo and Y. Wang, *Tissue Eng.*, 2006, **12**, 917-925.
 18. D. Motlagh, J. Yang, K. Y. Lui, A. R. Webb and G. A. Ameer, *Biomaterials*, 2006, **27**, 4315-4324.
 19. C. A. Sundback, J. Y. Shyu, Y. Wang, W. C. Faquin, R. S. Langer, J. P. Vacanti and T. A. Hadlock, *Biomaterials*, 2005, **26**, 5454-5464.
 20. Q.-Z. Chen, A. Bismarck, U. Hansen, S. Junaid, M. Q. Tran, S. E. Harding, N. N. Ali and A. R. Boccaccini, *Biomaterials*, 2008, **29**, 47-57.
 21. Q.-Z. Chen, H. Ishii, G. A. Thouas, A. R. Lyon, J. S. Wright, J. J. Blaker, W. Chrzanowski, A. R. Boccaccini, N. N. Ali and J. C. Knowles, *Biomaterials*, 2010, **31**, 3885-3893.
 22. G. C. Engelmayr, M. Cheng, C. J. Bettinger, J. T. Borenstein, R. Langer and L. E. Freed, *Nat. Mater.*, 2008, **7**, 1003-1010.
 23. Q.-Y. Liu, S.-Z. Wu, T.-W. Tan, J.-Y. Weng, L.-Q. Zhang, L. Liu, W. Tian and D.-F. Chen, *J. Biomater. Sci. Polym. Ed.*, 2009, **20**, 1567-1578.
 24. M. Martina and D. W. Hutmacher, *Polym. Int.*, 2007, **56**, 145-157.
 25. A. Patel, A. K. Gaharwar, G. Iviglia, H. Zhang, S. Mukundan, S. M. Mihaila, D. Demarchi and A. Khademhosseini, *Biomaterials*, 2013, **34**, 3970-3983.
 26. Y. T. Jia, W. Z. Wang, X. J. Zhou, W. Nie, L. Chen and C. L. He, *Polym. Chem.*, 2016, **7**, 2553-2564.
 27. X. Zhao, H. Wu, B. L. Guo, R. N. Dong, Y. S. Qiu and P. X. Ma, *Biomaterials*, 2017, **122**, 34-47.
 28. S. M. Choi, Y. Lee, J. Y. Son, J. W. Bae, K. M. Park and K. D. Park, *Macromol. Res.*, 2017, **25**, 85-91.
 29. Z. Wang, Y. Ma, Y. Wang, Y. Liu, K. Chen, Z. Wu, S. Yu, Y. Yuan and C. Liu, *Acta Biomater.*, 2018, **71**, 279-292.
 30. Y. B. Wu, L. Wang, B. L. Guo and P. X. Ma, *J. Mater. Chem. B*, 2014, **2**, 3674-3685.

31. W. M. Gramlich, I. L. Kim and J. A. Burdick, *Biomaterials*, 2013, **34**, 9803-9811.
32. Z. Muñoz, H. Shih and C.-C. Lin, *Biomater. Sci.*, 2014, **2**, 1063-1072.
33. H. W. Ooi, C. Mota, A. T. Ten Cate, A. Calore, L. Moroni and M. B. Baker, *Biomacromolecules*, 2018, **19**, 3390-3400.
34. B. D. Fairbanks, M. P. Schwartz, A. E. Halevi, C. R. Nuttelman, C. N. Bowman and K. S. Anseth, *Adv. Mater.*, 2009, **21**, 5005-5010.
35. A. K. O'Brien, N. B. Cramer and C. N. Bowman, *J. Polym. Sci. A Polym. Chem.*, 2006, **44**, 2007-2014.
36. A. D. Shubin, T. J. Felong, D. Graunke, C. E. Ovitt and D. S. Benoit, *Tissue Eng. Part A*, 2015, **21**, 1733-1751.
37. Q. Xu, C. He, C. Xiao and X. Chen, *Macromol. Biosci.*, 2016, **16**, 635-646.
38. J. J. Roberts and S. J. Bryant, *Biomaterials*, 2013, **34**, 9969-9979.
39. J. D. McCall and K. S. Anseth, *Biomacromolecules*, 2012, **13**, 2410-2417.
40. Y. C. Yeh, L. L. Ouyang, C. B. Highley and J. A. Burdick, *Polym. Chem.*, 2017, **8**, 5091-5099.
41. P. Pholpabu, S. S. Yerneni, C. Zhu, P. G. Campbell and C. J. Bettinger, *ACS Biomater. Sci. Eng.*, 2016, **2**, 1464-1470.
42. C. C. Lin, C. S. Ki and H. Shih, *J. Appl. Polym. Sci.*, 2015, **132**.
43. Z. Wang, Y. Cong and J. Fu, *J. Mater. Chem. B*, 2020, **8**, 3437-3459.
44. Z. Qiao, J. Parks, P. Choi and H.-F. Ji, *Polymers*, 2019, **11**, 1773.
45. S. Zhu, J. Wang, H. Yan, Y. Wang, Y. Zhao, B. Feng, K. Duan and J. Weng, *J. Mater. Chem. B*, 2017, **5**, 7021-7034.
46. L. Han, L. Yan, K. Wang, L. Fang, H. Zhang, Y. Tang, Y. Ding, L.-T. Weng, J. Xu and J. Weng, *NPG Asia Mater.*, 2017, **9**, e372-e372.
47. M. Zhu, Y. Liu, B. Sun, W. Zhang, X. Liu, H. Yu, Y. Zhang, D. Kuckling and H. J. P. Adler, *Macromol. Rapid Commun.*, 2006, **27**, 1023-1028.
48. G. Cai, J. Wang, K. Qian, J. Chen, S. Li and P. S. Lee, *Adv. Sci.*, 2017, **4**, 1600190.
49. E. M. Jeffries, R. A. Allen, J. Gao, M. Pesce and Y. Wang, *Acta Biomater.*, 2015, **18**, 30-39.
50. S. Mongkhontreerat, K. Öberg, L. Erixon, P. Löwenhielm, A. Hult and M. Malkoch, *J. Mater. Chem. A*, 2013, **1**, 13732-13737.
51. M. A. Daniele, A. A. Adams, J. Naciri, S. H. North and F. S. Ligler, *Biomaterials*, 2014, **35**, 1845-1856.
52. Y. Wang, Y. Li, X. Yu, Q. Long and T. Zhang, *RSC advances*, 2019, **9**, 18394-18405.
53. F. Yi and D. A. LaVan, *Macromol. Biosci.*, 2008, **8**, 803-806.
54. Y. C. Yeh, C. B. Highley, L. Ouyang and J. A. Burdick, *Biofabrication*, 2016, **8**, 10.

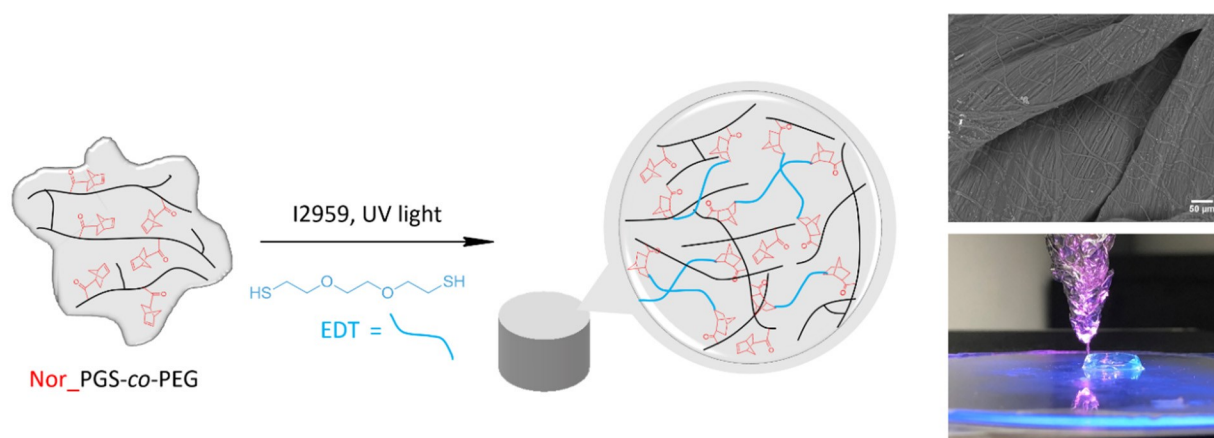
Table of contents

Formation of highly elastomeric and property-tailorable poly(glycerol sebacate)-co-poly(ethylene glycol) hydrogels through thiol-norbornene photochemistry

Yu-Ting Tsai,^a Chun-Wei Chang^a and Yi-Cheun Yeh*^a

^a Institute of Polymer Science and Engineering, National Taiwan University, Taipei, Taiwan

E-mail: yicheun@ntu.edu.tw



Nor_PGS-co-PEG is a new type of hydrophilic PGS-based copolymer with definable properties for scaffold manufacturing as well as for biomedical applications.

Supplementary information

Formation of highly elastomeric and property-tailorable poly(glycerol sebacate)-co-poly(ethylene glycol) hydrogels through thiol-norbornene photochemistry

Yu-Ting Tsai,^a Chun-Wei Chang^a and Yi-Cheun Yeh*^a

^aInstitute of Polymer Science and Engineering, National Taiwan University, Taipei, Taiwan

E-mail: yicheun@ntu.edu.tw

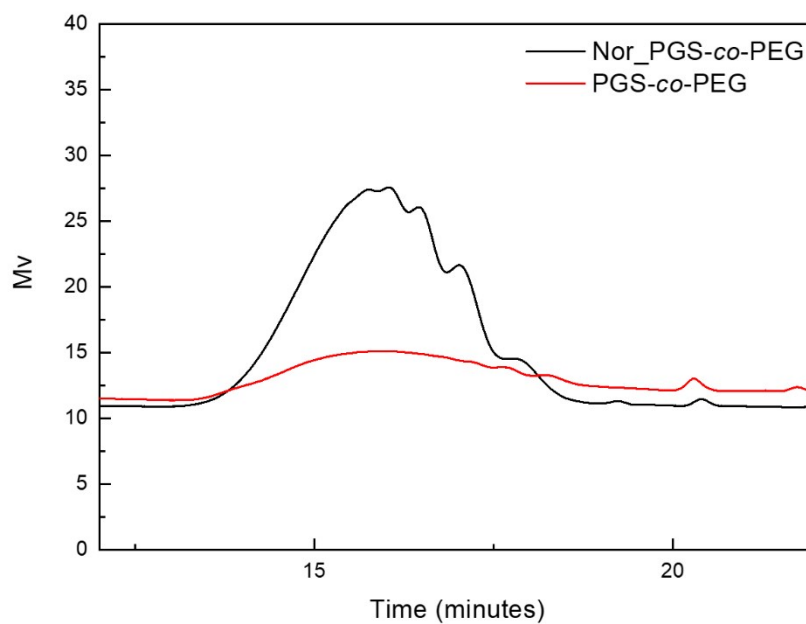


Fig. S1 GPC traces of PGS-co-PEG and Nor_PGS-co-PEG macromers. PGS-co-PEG: Mw= 8.8 kDa, PDI= 6.87; Nor_PGS-co-PEG: Mw= 9.6 kDa, PDI= 2.71.